A Fully Inkjet-Printed Chipless RFID Gas and Temperature Sensor on Paper

Arnaud Vena
Institut d'Electronique du Sud, UM2
Montpellier, France

Lauri Sydänheimo, Leena Ukkonen
Department of Electronics, TUT
Tampere, Finland

Manos M. Tentzeris
School of ECE, Georgia Tech
Atlanta, USA

Abstract— **This paper studies the implementation of an RFID chipless sensor based on split ring resonators. It operates in the ISM band at 2.45GHz to detect a change of carbon dioxide, and a variation of temperature. The realization of this passive wireless sensor involves inkjet printing using several ink types so that a device that works can be realized from scratch in a few stages. The substrates used are flexible materials to allow for seamless integration on any object shapes. Several samples have been printed on polyimide substrate 50 µm thick to validate the design with the help of wireless measurements. Finally, another set of samples printed on an ordinary cardboard of 550 µm thickness is realized and measured, and the performance achieved are compared with those of the polyimide based sensors.**

Keywords—chipless sensor, RFID, gas, temperature, paper, inkjet-printing, carbon nanotubes

I. INTRODUCTION

Radio Frequency Identification is a technology of identification spread worldwide, which uses the propagation of the electromagnetic (EM) waves for the sake of remote detection [1]. The key advantages that make it famous to compare with other technologies of identification, such as the optical barcode is its ease of detection and a comfortable read range up to several meters. Moreover, compared to classical RF transponders involved in standard wireless communication links, passive RFID tags do not require any battery cell. Indeed, in this case, the chip is empowered by the EM field radiated by the reader. This reduces the maintenance cost of this family of RFID tags to zero, therefore increase considerably their life duration. Besides, novel applications are appearing to perform an ever increasing number of daily tasks. For several years, adding a sensing functionality to a RFID tag has been studied [2-3]. The potential applications are, in the field of air quality detection, health, and food traceability from the supplier until the customer. The use of RFID enabled sensors can be very judicious, except that the unit cost of a RFID tag is still too high in some applications for a large deployment.

The missing link between the RFID technology and the optical barcode is called chipless RFID or RF barcode [4-9] and the basic principle is depicted in Fig. 1. It relies upon the detection of the static backscattered EM response of resonant scatterers. Both the magnitude of the peak and its resonant frequency can be used for coding and sensing purposes. Researches in this field are getting more intense for over the last years, mainly in the field of chipless RFID sensors. The advantages of a chipless device is its lower cost (< 1 $ cent in [9]) compared to that of a chipped RFID tag for a coding capacity which can reach more than 40 bits with low k substrate. They can be realized in a single step using printing techniques as they eliminate the need to attach a chip to the antenna, that commonly complicates the fabrication of conventional tags. Though numerous challenges still exist for the realization of reliable and cheap interrogation systems, chipless sensors [10-15] could potentially be one of the best solutions for a large-scale deployment for pervasive sensing.

In this paper we study the realization of fully inkjet printed chipless sensors on paper that can be used to track changes of CO_2 or temperature (see Fig. 2 (a) and (b)). For this purpose we use a commercial conductive ink and a commercial resistive ink based on single walled carbon nanotubes (SWCNTs), that is sensitive to several physical parameters, and we realized the
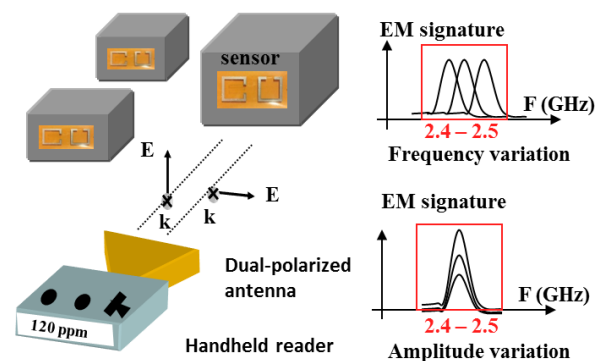

Figure 1.   Basic principle of passive chipless wireless detection.

sensors on flexible laminates. A first set of samples was made on polyimide substrate, whereas the second set of samples was realized on a commonly used cardboard of 550 μm thickness. In [15], a similar design printed on polyimide substrate has been successfully employed for smoke detection. In this work we improved the setup in order to find out which of the temperature, the CO2, the CO, or the humidity is mainly detected with the proposed chipless sensor. In Section I, we present the basic principles and the design process of the chipless sensor. Then, in Section II we present the wireless measurements obtained for both polyimide-based substrate and paper-based substrate sensors. Before concluding, we discuss about the concept of a reading system that could be potentially utilized for the practical implementation of this sensing technology.

II. PRINCIPLE OF THE APPLICATION

A. Electromagnetic properties

The operating principle of a chipless sensor is very close to a radar detection application. The idea is to detect and record its EM signature that is dependent on the chosen physical parameters. Unlike chipped RFID there is no variable load to modulate the incident field in order to generate two distinct levels of backscattered power. Thus, for a given incident power, a constant value of a sensed physical parameter, the backscattered response is static. This means that, to extract the EM signature of the tag, the measurement of the ambient backscattering in the absence of the tag has to be measured and subtracted from the overall backscattered signal when the RFID is interrogated.

The sensor used in this paper is shown in Fig. 2 (a) and (b). It is based on a well known shape that is based on dual polarization squared single split ring (SRR) resonators. This shape has already been used in [15] for smoke detection. The dimensions of the design are given in Fig. 3 (a). The width of
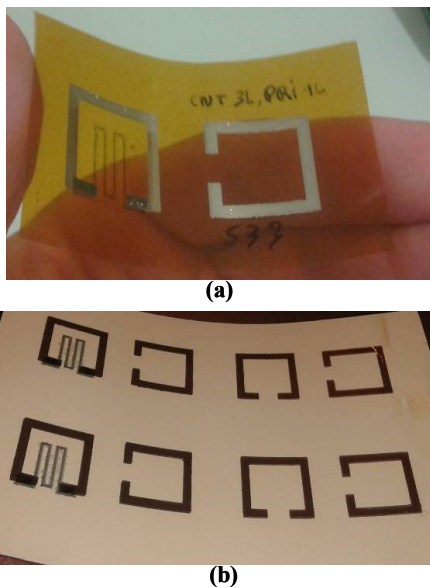

(a)

(b)

Figure 2. View of the design (a) printed on polyimide, (b) printed on commonly used cardboard with a thickness of 550 μm.
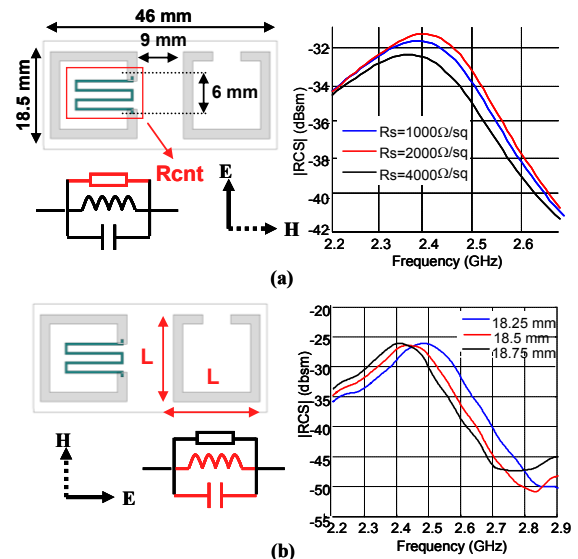

(a)

(b)

Figure 3. Coding principle. (a) Magnitude variation correlated with the concentration of a gas or the temperature, in vertical polarization. (b) Frequency shift to encode an identifier, in horizontal polarization.

the conductive strip is 2 mm, and the width of the meandered resistive strip bridging the two edges of the capacitor is 0.75 mm, for a total length of 54 mm. The present work shows new results compared to [15] concerning the temperature detection as well as measurement results for a cardboard based sensor. When an incident EM wave impinges on the scatterer, part of the energy is directly reflected backward to the source and the rest remains localized in the RFID resonator exciting several resonant modes. In this case the energy is released slowly with a duration that depends on the quality factor of the resonator. Designing an efficient chipless sensor consists in generating a resonant mode that is strongly dependant on a physical parameter. Typically either the magnitude of this mode or its frequency, or both, is the variable correlated with the parameter to sense as shown in Fig. 1 (c). The design shown in Fig. 2 is designed to operate at 2.45 GHz. A resonant peak can be detected when the device is subjected to a vertically, or a horizontally polarized incident wave.

B. Coding principle

Based on the spectrum analysis of the EM response of the sensor we can extract an identifier (ID) and information correlated with the concentration of a gas or the temperature variation. For the current design we decided to use the EM response in vertical polarization for sensing purposes. The horizontal polarization EM response is used to encode an ID and as a reference scatterer. Each scatterer can be roughly modeled by a parallel resonant circuit for which either the resistance part or the capacitor/inductor value is varying as a function of the sensed parameter.

As shown in Fig. 3 (a), the coding of the sensed parameter relies upon the variation of the magnitude of the resonant peak due to the variation of the sheet resistance of the CNT based ink deposit. The initial value is 1000 Ω/sq at 25°C, for an ambient CO_2 concentration of 500 ppm. When the sensor is subjected to CO_2 gas or when the temperature rises, this value

tends to rise. As a result, the peak magnitude of the reflected EM signature increases. To obtain a value independent from the reading range, this magnitude is normalized by the peak magnitude of the orthogonally polarized response shown in Fig. 3 (b).

Besides, to encode the ID with the horizontally polarized EM response, we modify the length *L* of the scatterer. In terms of electrical equivalent circuit, this means that both the capacitor and inductor are modified so that the resonant frequency is shifted. The example of the Fig. 3 (b) shows three different resonant frequencies that can be detected within the ISM band from 2.4 GHz to 2.5 GHz. Thus three different IDs can be encoded for a single resonator.

C. Realization and material

We realized several samples with the help of an inkjet printer Dimatix DMP-2831 shown in Fig. 4 (a). The first stage consists in printing the conductive parts of the sensor using commercial silver ink Harima Nanopaste, followed by a sintering at 150°C during one hour. Then we print the sensitive meander between the two arms of one SRR using a composite ink Poly-ink [16] based on PEDOT-PSS loaded by SWCNTs. It is noteworthy that no sintering is required for this ink. This material has been chosen for its great properties to detect various gases [17]. Indeed, gas molecules which get into contact with CNTs are subject to physical adsorption so that they get trapped into the lattice. Adsorption can happen on the surface of the nanotube or inside. As a result, the conductivity of each CNT which has trapped gas molecules is modified. At the macroscopic scale, we observe a significant sheet resistance variation as a function of the gas concentration. From the electromagnetic side, a resonator loaded with a varying sheet resistance is reflecting a varying power well correlated with the gas concentration.

The first realizations are made on polyimide substrate with 50 µm of thickness (see Fig. 2 (a)), with permittivity εr=3.5, tanδ=0.0027. Then to study the behavior of the proposed sensor topologies on low-cost versatile materials, prototypes have been fabricated on cardboard with a thickness of 550 um as shown in Fig. 2 (b). The measured permittivity for this substrate is εr=3, tanδ=0.03. With silver ink, the sheet resistance achieved on polyimide substrate is 0.5 Ω/sq for two layers printed at 635 dpi, whereas on cardboard with 550 µm of thickness, with four layers we get 1 Ω/sq. The achieved sheet resistance measured with CNT-based ink is approximately equal to 450 Ω/sq for three layers printed at 1693 dpi.

III. WIRELESS MEASUREMENT RESULTS

To validate the sensors we measured their EM signature when subjected to a high concentration of carbon dioxide (20000 ppm), and then when the temperature varies from 53°C to 27°C. The sensors are set inside an air tight box as shown in Fig. 4 (b), placed at 20 cm in the front of a dual-polarization antenna. Inside the box, a probe Delta Ohm HD37AB17D records the CO_2 and CO concentration, the temperature, and the relative humidity. The box can be filled with either pure CO_2 or dry air. To measure the EM response of the sensor, we use a dual-polarization antenna ETS Lindgren 3164-04 having
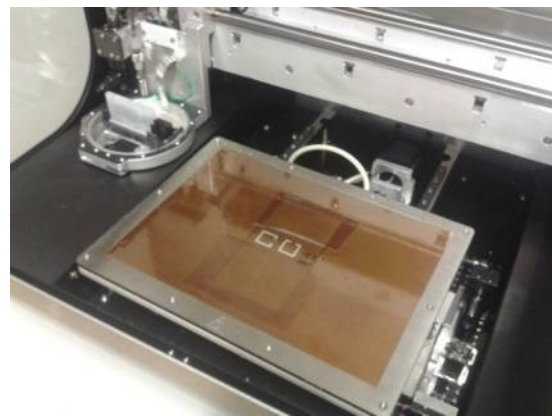
(a)
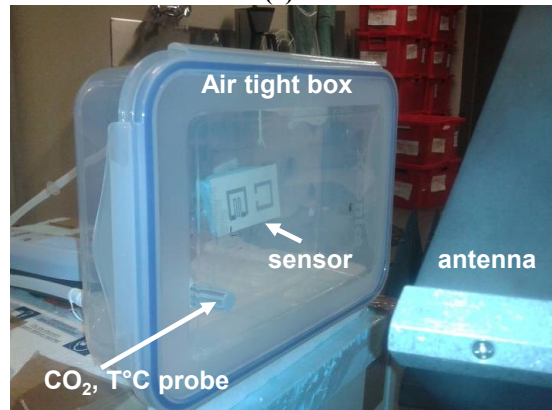
(b)

Figure 4. (a) View of the realized silver-based printed scatterers in the Dimatix DMP-2831 printer (b)View of the measurement setup for gas and temperature detection.

a gain close to 9 dBi at 2.45 GHz, connected to a vector network analyzer (VNA). From the raw measurements of the VNA in terms of S parameters S11 and S22, we can extract the radar cross section (RCS) of the sensor provided a calibration is done [9].

A. Results of sensors realized on polyimide substrate

We measure first, the sensitivity of the printed polyimide-based sensor when subject to a large concentration of CO_2, that is, 20000 ppm. The box is filled with only one short discharge (the gas supply is opened during approximatelly 1 s). The curve shown in Fig. 5 shows the recorded concentration of CO_2 as a function of the time all along the test. Figures 6 (a) and (b), show the difference between the initial response, and the final response of the sensor in horizontal, and vertical polarization, respectively. We note a 0.5 dB magnitude change for the vertically polarized response, whereas no significant variation is shown in horizontal polarization. This proves the good sensitivity of the CNT-based deposit for which the resistivity is varying as a function of the CO_2 concentration. The Fig. 7 shows the extracted relative magnitude variation, for the resonant peak, in vertical polarization for two different samples realized the same way. The behavior is similar in both cases. We see a sharp variation just after CO_2 injection followed by a constant value that lasts even if the CO_2 concentration returns to a lower value. This behavior is typically due to the
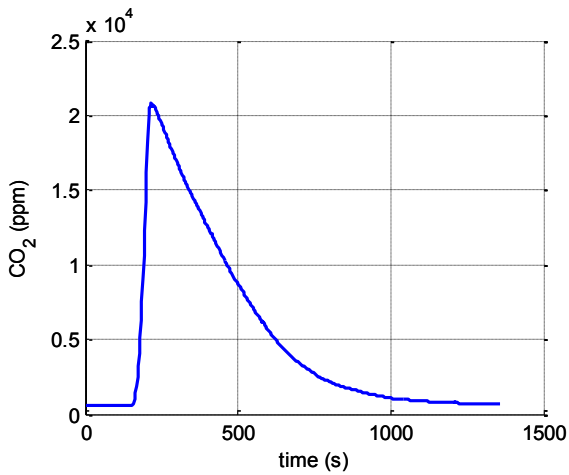
Figure 5. CO_2 concentration inside the box recorded all along a measurement cycle by a probe Delta Ohm.

adsorption of gas molecules by CNTs which get trapped. One way to release these molecules is to use UV light or to clean the sensor with nitrogen (N_2). It is noteworthy that the magnitude variation is close to 0.5 dB for the two different
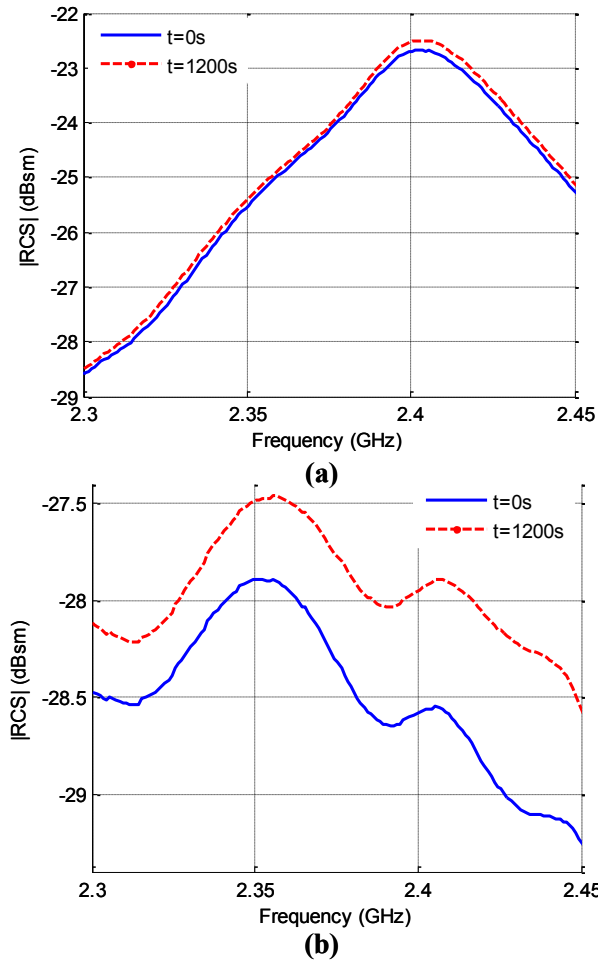

(a)

(b)

Figure 6. Measured RCS of the printed sensor on polyimide before and after injection of CO_2 inside the test chamber (a) in horizontal polarization, (b) in vertical polarization.
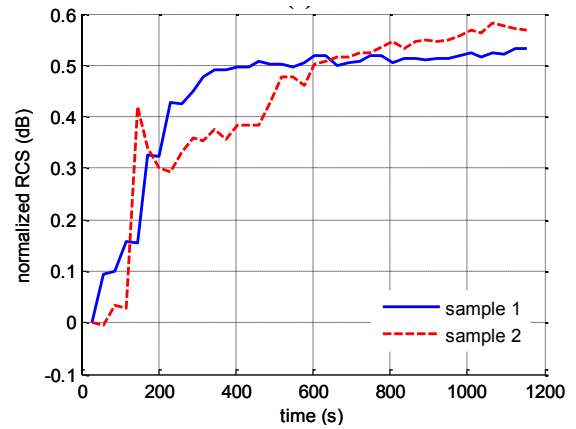

Figure 7. Measured RCS variation in vertical polarization of the resonant peak for two sensors subject to CO_2. The samples have been printed on polyimide substrate the same way.

samples.

In a second stage we seek extracting a relationship between the temperature and the magnitude variation of the reflected responses of the sensor. For this purpose we heat the air within the box using a hot air blower to reach a temperature close to 60°C. Then, we record the magnitude variation from this temperature to the ambient temperature. The Fig. 8 shows the normalized RCS variation in vertical polarization for the two aforementioned samples. The two curves are very close, and the magnitude variation is 2 dB for a 26°C difference. Contrary to the CO_2 detection behavior, the magnitude variation of the reflected response is linearly correlated with the temperature variation. This point is verified by the temperature profile recorded by the probe and shown in Fig. 8. The profile is very close to the shapes of the measured RCS curves.

B. Results of sensors realized on carboard

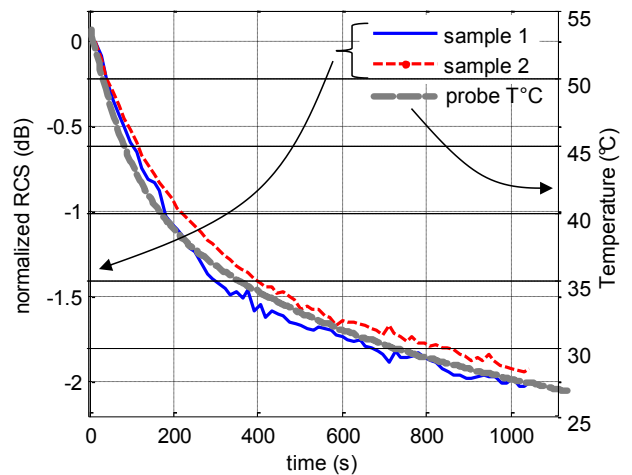The last set of results reported in this study concerns the

Figure 8. Measured RCS variation in vertical polarization of the resonant peak for two sensors when the temperature is varying from 53°C to 27°C. The samples have been printed on polyimide substrate the same way. The temperature inside the box has been recorded all along the measurement cycle by a probe Delta Ohm.
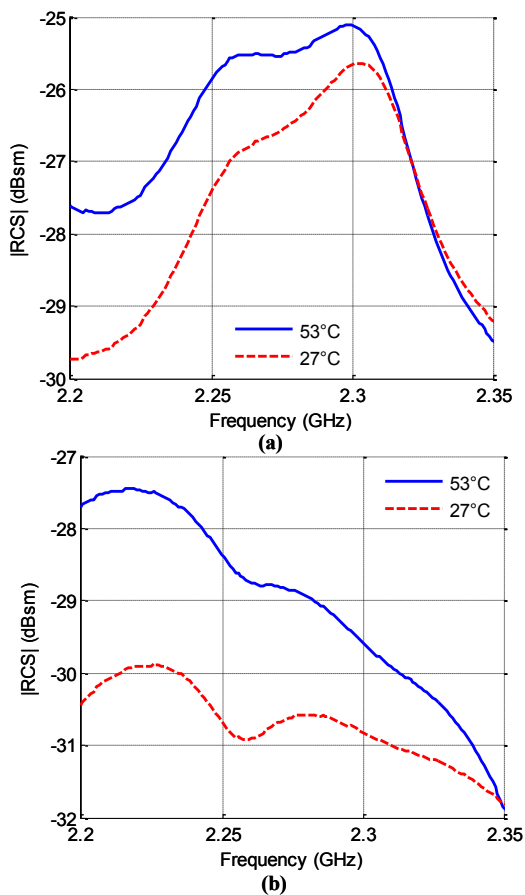
Figure 9. Measured RCS of the printed sensor on cardboard with 550 µm of thickness subject to a temperature variation inside the test chamber (a) in horizontal polarization, (b) in vertical polarization.

measurement of the reflected response of a sensor printed on a commonly used cardboad substrate. Measurements of the sensor subject to a large CO_2 concentration has not shown significant magnitude changes on the reflected response. This result is most likely due to the deeper diffusion of the ink within the paper so that gas molecules more hardly get into contact with the sensitive surface. A surface treatment as well as an increased number of layer may solve this issue. However, temperature measurements showed a quasi similar behavior to that of the polyimide based sensor. Figures 9 (a) and (b) show the EM response in horizontal and vertical polarization, respectively. We can observe a deviation for the two polarizations, however, the vertically polarized response shows a much larger magnitude difference, that is 2.5 dB, as plotted in Fig. 10 (a). Based on these curve we can extract the relationship between the normalized RCS variation and the temperature as in Fig. 10 (b) for the two polarizations. The obtained result shows a linear behavior at least within the range 53°C to 27°C. This verifies the capability to implement a fully printed sensor on a low cost substrate that is paper, at least for temperature variation detection.

IV. DISCUSSION ON THE READING SYSTEM

Before concluding this study we discuss about the concept of a reading system that could be implemented in order to
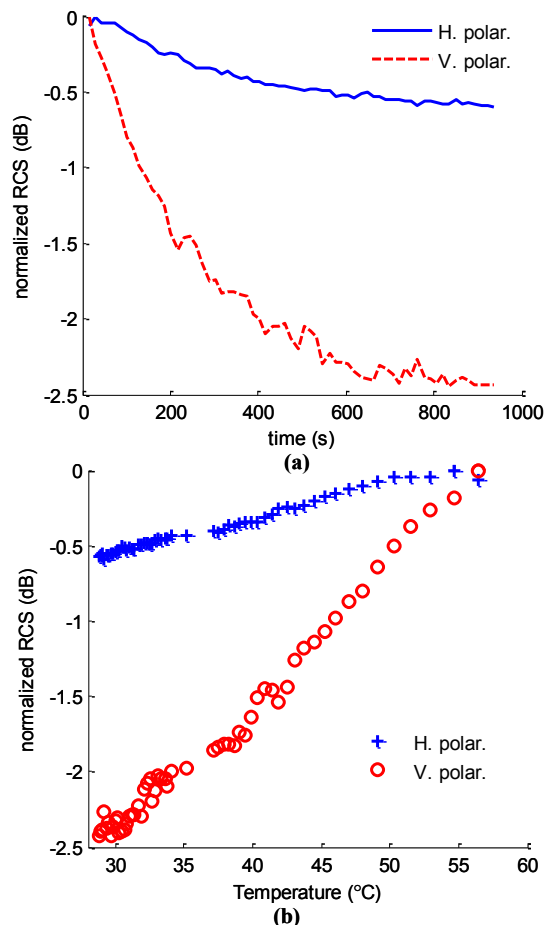

Figure 10. .(a) Measured RCS variation of the resonant peak in both polarizations when the temperature is varying from 53°C to 27°C. The sensor under test has been printed on cardboard of 550 µm of thickness. (b) Extracted relationship in both polarization between the normalized magnitude at the resonant peak and the temperature.

practically interrogate the proposed sensor. The operating frequency is centered on the ISM band at 2.45 GHz so that the usable frequency bandwidth is between 2.4 GHz and 2.5 GHz. In order to sense the EM signature of the sensor for these frequencies we can implement a frequency-stepped continuous wave (FSCW) radar similar to that in [18] for which the basic principle is depicted in Fig. 11. This technique relies upon the use of a voltage controlled oscillator (VCO) to generate a frequency sweep at the source. An amplifier could be present
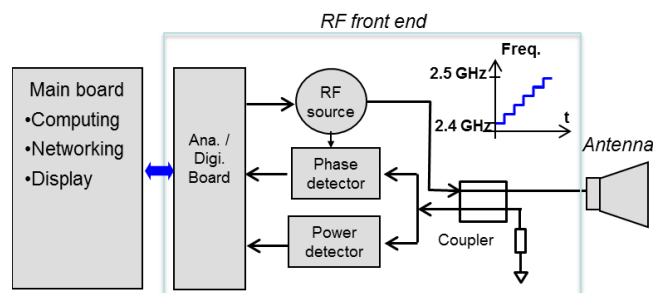

Figure 11. Architecture of a detection system using a FSCW radar technique to read chipless sensors within the ISM band at 2.45GHz.

after the VCO in order to reach the maximum allowable radiated power that is 36 dBm for the considered frequencies. In the receiver stage, a mixer can be used to downconvert the received signal frequency before detecting its power and its phase. It should be noted that a small part of the transmitted signal is used to detect the phase of the received EM response. An alternative relies upon the implementation of frequency-modulated continuous wave radar (FMCW), that has been successfully tested in [12]. Still, the calibration stage based on the measurement of the background and of a reference object is of upmost importance in order to extract the correct sensor response.

V. CONCLUSION

We presented the design of a fully inkjet printed sensor and showed its realization on two different flexible laminates that are polyimide and cardboard. For this purpose, we utilized two different commercial inks in order to realize first, highly conductive stripes for scattering/radiation, and second, resistive strips based on CNT as sensing material. Radar measurements have validated the feasibility of the sensor realized on polyimide substrate as a CO_2 threshold sensor or a temperature sensor. Moreover, the first tests carried out on a printed sensor on cardboard verified the proof of concept of a very low cost sensor that can be used for temperature detection featuring a linear relationship of the normalized RCS with temperature. The next step is to develop the concept of paper based sensor to extend this concept to paper-based gas sensors.

REFERENCES

[1] D. M. Dobkin, "The RF in RFID, Passive UHF RFID in Practice", Newnes, 2008.

[2] S. Manzari, C. Occhiuzzi, S. Nawale, A. Catini, C. Di Natale, G. Marrocco, "Polymer-doped UHF RFID tag for wireless-sensing of humidity," *IEEE Int. Conf. on RFID*, Orlando, April 2012, pp. 124-129.

[3] R. Bhattacharyya, C. Floerkemeier, S. Sarma, D. Deavours, "RFID Tag Antenna Based Temperature Sensing in the Frequency Domain," *IEEE Int. Conf. on RFID*, 2011, pp. 70-77.

[4] R. Nair, E. Perret & S. Tedjini, "Temporal multi-frequency encoding technique for chipless rfid applications," *Microwave Symposium Digest (MTT), 2012 IEEE MTT-S International*, pp. 1-3, 2012.

[5] J. McVay, A. Hoorfar, and N. Engheta, "Space-filling curve RFID tags," *Proc. 2006 IEEE Radio and Wireless Symp.*, San Diego, CS, pp. 17-19.

[6] S. Preradovic, N. C. Karmakar,"Multiresonator based chipless RFID tag and dedicated RFID reader," *IEEE MTT-S International Microwave Symposium Digest*, Anaheim, CA, May 2010, pp. 1520-1523.

[7] H-S Jang, W-G Lim, K-S Oh, S-Mo Moon and J-W Yu, "Design of Low-Cost Chipless System Using Printable Chipless Tag With Electromagnetic Code," *IEEE Microwave and Wireless Components Letters*, vol.20, no.11, pp.640-642, Nov. 2010.

[8] F. Costa, S. Genovesi, A. Monorchio, "A Chipless RFID Based on Multiresonant High-Impedance Surfaces," *IEEE Transactions on Microwave Theory and Techniques,* vol.61, no.1, pp.146,153, Jan. 2013.

[9] A. Vena, E. Perret, S. Tedjini, G. Eymin-Petot-Tourtollet, A. Delattre, F. Garet, Y. Boutant, "Design of Chipless RFID Tags Printed on Paper by Flexography," *IEEE Transactions on Antennas and Propagation*, vol.PP, no.99, pp.1-10.

[10] L. Yang, R. Zhang, D. Staiculescu, C. P. Wong and M. M. Tentzeris, "A novel conformal RFID-enabled module utilizing inkjet-printed antennas and carbon nanotubes for Gas-Detection Applications," *IEEE Antennas and Wireless Propagation Letters*, Vol. 8, 2009, pp. 653-656.

[11] T. Thai, F. Chebila, J. Mehdi, P. Pons, H. Aubert, G. Dejean, M. Tentzeris and R. Plana, "Design and development of a millimetre-wave novel passive ultrasensitive temperature transducer for remote sensing and identification," *Microwave Conference (EuMC), 2010 European*, 2010, pp. 45-48.

[12] A. Traille, S. Bouaziz, S. Pinon, P. Pons, H. Aubert, A. Boukabache, M-M. Tentzeris, "A Wireless Passive RCS-based Temperature Sensor using Liquid Metal and Microfluidics Technologies," *European Microwave Week*, Manchester, 2011.

[13] E. M. Amin, S. Bhuiyan, N. Karmakar, B. Winther-Jensen, "A novel EM barcode for humidity sensing," *IEEE International Conference on RFID*, pp.82-87, April 30 2013-May 2 2013.

[14] C. Mandel, M. Schüßler and R. Jakoby, "A wireless passive strain sensor," *IEEE Sensors Journal*, pp.207-210, 28-31 Oct. 2011.

[15] A. Vena, L. Sydänheimo, M. M. Tentzeris, L. Ukkonen, "A Novel Inkjet Printed Carbon Nanotube-Based Chipless RFID Sensor for Gas Detection," *European Microwave Week 2013*, Nuremberg, Germany October 6-11, 2013 (accepted).

[16] Poly-Ink, http://www.poly-ink.fr/.

[17] Y. Wang and J. T. W. Yeow, "A Review of Carbon Nanotubes-Based Gas Sensors," Journal of Sensors, vol. 2009, Article ID 493904, 2009.

[18] S. Preradovic, N.C. Karmakar and M. Zenere, "UWB chipless tag RFID reader design," *IEEE International Conference on RFID-Technology and Applications (RFID-TA)*, Guangzhou, China, pp.257-262, 17-19 June 2010.